



Addressing the relocation bias in a long temperature record by means of land cover assessment

Isabel Knerr^{1,2} · Manuel Dienst² · Jenny Lindén³ · Petr Dobrovolný⁴ · Jan Geletic⁵ · Ulf Büntgen^{4,5,6} · Jan Esper²

Received: 13 July 2018 / Accepted: 15 January 2019 / Published online: 25 January 2019
© Springer-Verlag GmbH Austria, part of Springer Nature 2019

Abstract

The meteorological measurements in Brno, Czech Republic, is among the world's oldest measurements, operating since 1799. Like many others, station was initially installed in the city center, relocated several times, and currently operates at an airport outside the city. These geographical changes potentially bias the temperature record due to different station surroundings and varying degrees of urban heat island effects. Here, we assess the influence of land cover on spatial temperature variations in Brno, capitol of Moravia and the second largest city of the Czech Republic. We therefore use a unique dataset of half-hourly resolved measurements from 11 stations spanning a period of more than 3.5 years and apply this information to reduce relocation biases in the long-term temperature record from 1799 to the present. Regression analysis reveals a significant warming influence from nearby buildings and a cooling influence from vegetation, explaining up to 80% of the spatial variability within our network. The influence is strongest during the warm season and for land cover changes between 300 and 500 m around stations. Relying on historical maps and recent satellite data, it was possible to capture the building densities surrounding the past locations of the meteorological station. Using the previously established land cover–temperature relation, the anthropogenic warming for each measurement site could be quantified and hence eliminated from the temperature record accordingly, thereby increasing the long-term warming trend.

1 Introduction

High-quality, long-term meteorological measurements form the backbone of modern climate research (Auer et al. 2005), including proxy-based paleoclimatology (Esper et al. 2007) and model-based climate change prediction and evaluation (e.g., Cox et al. 1999; Leach 2007; Voltaire et al. 2012). The term

high quality implies that the data is homogenous, i.e., variability and trends are exclusively caused by weather and climate (Aguilar et al. 2003; Venema et al. 2012b). Even though continuous efforts to reduce non-climatic biases in meteorological measurements are improving data homogeneity, biases due to changes in observing practices, instrumentation, or station surroundings are found in long station records (Auer et al. 2005; Brunet et al. 2006a; Moberg and Bergström 1997). Many studies report that the most important inhomogeneities are related to station relocations and its implications, i.e., a change in site conditions and hence microclimate (e.g., Brunet et al. 2006a; Rahimzadeh and Zavareh 2014; Tuomenvirta 2001).

The oldest meteorological stations were often originally placed within cities to ensure good accessibility, but these cities gradually grew to become larger and were modernized, frequently leading to changes in station surroundings and thus triggering relocations (Allen et al. 2011). The potential influence of an urban-induced temperature trend in these records has been examined in numerous studies (e.g., Goodridge 1992; Jones et al. 2008; Parker 2010; Portman 1993; Wigley and Santer 2013). The main concern is the influence of the urban heat island—the warming effect caused by limited radiative and advective cooling due to urban geometry, increased thermal admittance of construction materials, reduced latent heat storage as a result of sealed surfaces, and limited

✉ Isabel Knerr
isabel.knerr@geo.uni-marburg.de

¹ Laboratory for Climatology and Remote Sensing, Department of Geography, Philipps-University Marburg, Deutschhausstraße 10, 35032 Marburg, Germany

² Department of Geography, Johannes Gutenberg-University, Mainz, Germany

³ IVL – Swedish Environmental Research Institute, Gothenburg, Sweden

⁴ Department of Geography, Masaryk University, Brno, Czech Republic

⁵ Institute of Computer Science, Czech Academy of Sciences, Brno, Czech Republic

⁶ Department of Geography, University of Cambridge, Cambridge, UK

vegetation coverage (Arnfield 2003). Studies have shown that differences in land cover can explain a significant part of the spatial variability in temperatures, not only with regard to urban/rural differences but also among urban sites per se (Chen et al. 2006; Lindén 2011). Although the thermal source area influencing temperatures can extend upwind for meters to kilometers (Stewart and Oke 2012), the most effective influences occur within 500 m horizontal distance or less in urban environments (Hart and Sailor 2009; Li and Roth 2009; Lindén 2011; Yokobori and Ohta 2009).

In order to reduce inhomogeneities in long time-series of meteorological observations (e.g., Auer et al. 2007; Begert et al. 2005), homogenization methods are often applied (Brunet et al. 2006b; Štěpánek et al. 2009), with ACMANT, CLIMATOL, or HOMER being some popular examples (Pérez-Zanón et al. 2015; Venema et al. 2012a). These approaches integrate statistical tests to identify break points and use relative homogenization approaches to compare one candidate time series with other records from nearby stations (Vincent 1998; Zhen and Zhong-Wei 2015). However, temperature records that cover more than 100 years or more are seldom and rarely close to nearby stations with records of similar length, thus restricting possibilities for relative homogenization. Alternative methods are therefore needed to assess and correct potential biases due to station relocations and other factors. Any attempt to do so relies on the availability of metadata in order to understand and consider the station history (Aguilar et al. 2003). Crucial information includes observation hours, relocation dates, changes in instrumentation, and environment.

Here, we assess the influence of land cover and other factors on spatial temperature differences in and around Brno, the second largest city of the Czech Republic. We therefore use a 3.5-year-long network of daily measurements from 11 stations in different urban and sub-urban environments. Our findings allow us to assess past temperature patterns in Brno based on historical maps. By considering former locations of old meteorological stations, the land cover analysis enables quantification of the urban heat island effect at each of these sites at different points in time. To correct for relocation biases in Brno's climate record, site-specific effects are removed from the original time-series, presumably allowing for an enhanced view on warming within the last two centuries.

2 Methods

2.1 Study area

Brno is located in the south-east of the Czech Republic in southern Moravia. Even though most part of the city extends within a basin, huge differences in altitude of more than 250 m occur between different parts of the urban area due to the

otherwise hilly terrain. Considering the Köppen climate classification (Peel et al. 2007), Brno exhibits a mixture of oceanic, temperate (Cfb), and humid continental climate (Dfb), with cold winters and warm summers. The average annual precipitation is 509 mm and the average annual air temperature is 9.3 °C based on the period from 1961 until 1990 (Brázdil et al. 2006).

2.2 Measurements

We use a network of 11 meteorological stations in the city of Brno to quantify spatial temperature differences. The network was established by the Masaryk University in Brno in cooperation with the Czech Hydrometeorological Institute (Dobrovolný et al. 2012). Since several studies reveal a distinct influence on station readings in a radius of 500 m or less (e.g., Chow and Roth 2006; Li and Roth 2009; Lindén et al. 2015), the dominating land surface within 500 m radius was first considered to assign the stations to three different descriptive classes based on the percentage of sealed areas surrounding the stations in order to evaluate whether an urban heat island (UHI) is existent in Brno (Fig. 1; Table 1).

The first class contains two urban stations in the historical city center with more than 75% of sealed areas, the second class includes three rural stations outside of the city with 40% or less of sealed areas, and the third class consists of six suburban stations with a percentage of sealed areas between 41% and 75%, all within a radius of 500 m around the measurement stations. Sites and classifications of the stations are displayed in Fig. 1, along with the locations of the historical station setup through time (Table 4). A countercheck relying on the local climate zones introduced by Stewart and Oke (2012) revealed the classification based on digitization matches the given categories very well (Table 2).

Temperatures were recorded at 10-min intervals from June 2011 to February 2015. A total of 35 days were missing in the final dataset, though all stations still reach a data coverage > 96%. Daily mean temperature was calculated by means of the arithmetic means based on measurements with a 10-min resolution. A determination of daily maximum and minimum temperatures was performed by selecting the highest and lowest 10-min values per day. Because of the intricacy that is inherent to an altitude correction for minimum and maximum values (Unwin 1980), these values have not been processed. Seasonal means were determined using the arithmetic mean of the daily values, whereas for minimum and maximum, the median was considered to reduce the influence of extremes. The seasonal means were correlated against all types of land cover within each radius considered (50 m, 100 m, 300 m, 500 m, 800 m, and 1000 m) to determine the most influential source area and land cover types. In order to estimate the amount of temperature change associated to land cover, a regression analysis was performed.

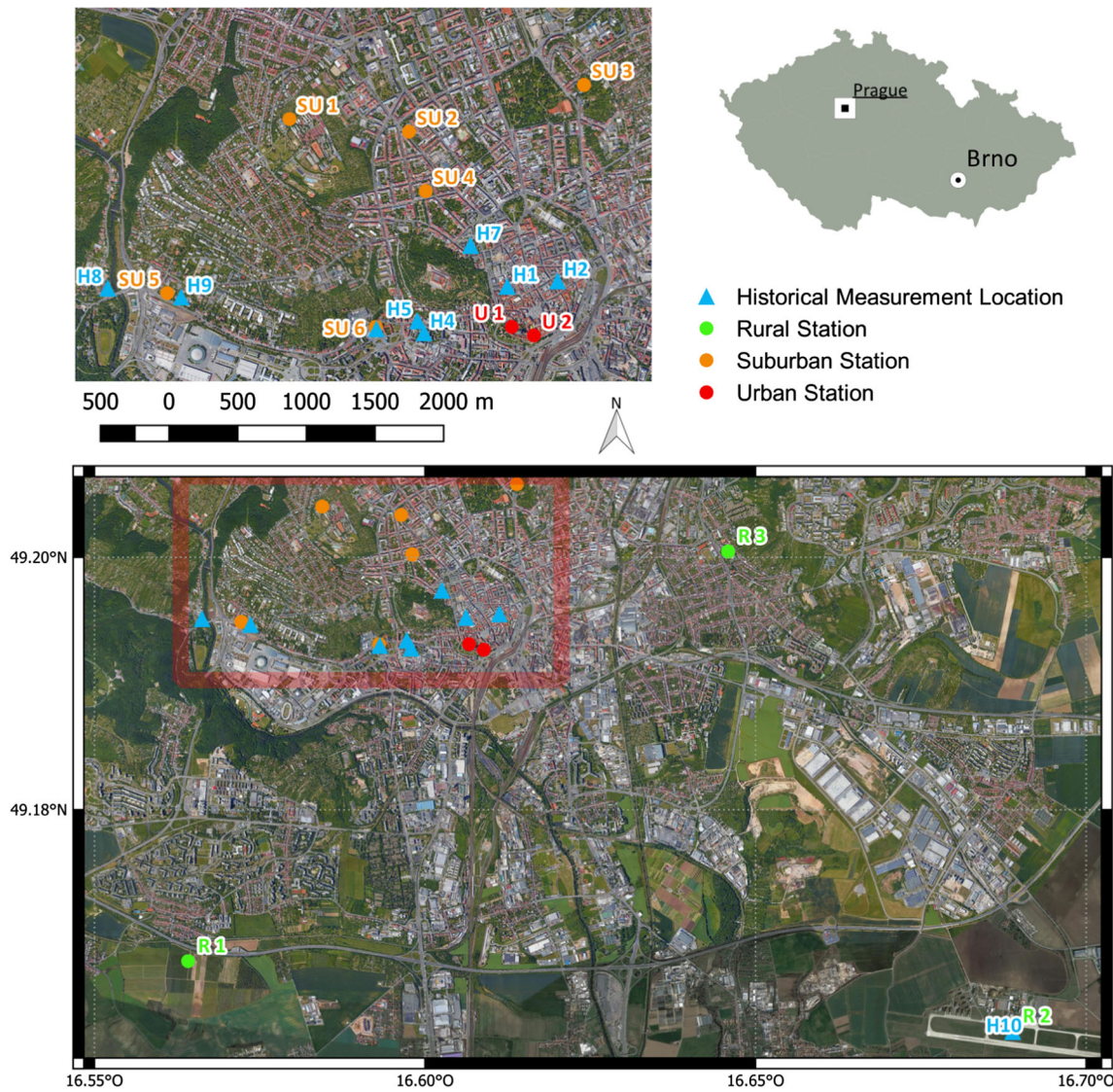


Fig. 1 Location of the 11 current measurement stations and historical measurement sites in the area of Brno. H3 is not shown because the exact location is not known

To better clarify whether certain sites are distinctly warmer or cooler than others, ΔT was used in the first analysis instead of absolute values. The ΔT values were calculated according to Eq. 1:

$$\Delta T_i = T_i - T_{\text{Rural}} \tag{1}$$

with T_{Rural} being the average of the temperature values for the rural stations used in the analysis and T_i ($i = 1 \dots 11$).

By means of Eq. 1, boxplot diagrams were created to detect a possible UHI effect as well as to check the distribution of the data available. Student's t test was performed to assess whether differences between the three categories of station groups

Table 1 Classification of land cover types in the wider area of Brno

Buildings*	All building structures
Paved areas*	Impermeable surfaces
Low vegetation**	Agricultural fields, gardens, meadows, and similar
High vegetation**	Forests, but also visible grove in gardens or along streets

*Combined in the category “sealed areas”

**Combined in the category “total vegetation”

Table 2 Climate stations and their locations in various local climate zones in the area of Brno

Name	Coordinates		Elevation (m a.s.l.)	Local climate zones
	LAT	LON		
U 1	49.191389	16.606667	245	Compact midrise (2)
U 2	49.190833	16.608889	227	Compact midrise (2)
R 1	49.16	16.564167	244	Sparsely built (9)
R 2	49.153056	16.688889	241	Large low-rise with low plants (8D)
R 3	49.200556	16.645833	216	Sparsely built (9)
SU 1	49.205	16.584444	298	Open midrise (5)
SU 2	49.204167	16.596389	242	Open midrise (5)
SU 3	49.207222	16.613889	225	Open midrise (5)
SU 4	49.200278	16.598056	234	Open midrise (5)
SU 5	49.193611	16.572222	214	Open midrise (5)
SU 6	49.191389	16.593056	206	Open midrise (5)

(rural, suburban, and urban) and their seasonal temperatures are significant on a 0.05 level.

2.3 Land cover change

To investigate the influence of land cover change to temperature regime in Brno, areas within a radius of 50 m, 100 m, 300 m, 500 m, 800 m, and 1000 m around the measurement stations were digitalized, using ArcGIS 10.3 and aerial photographs. The settlement structure and density was classified into six representative categories in order to include the most important land cover types, though two of these (water bodies, gravel/sand) were excluded from the analysis due to insignificant occurrences. An overview of the remaining four classes and an additional combination into “sealed areas” and “total vegetation” are shown in Table 1.

Especially in cities, a subdivision between low and high vegetation is important as their influence on air temperature may be different. Depending on the moisture content, large areas with low vegetation might absorb heat during day and emit it during night, similar to paved surfaces, i.e., these areas do not necessarily contribute to cooling (Taha 1997; Wang et al. 2016). Since a differentiation between low and high vegetation solely by interpreting an aerial photo is difficult, the combined category “total vegetation” was generated. To quantify the aggregated warming effect of buildings and paved areas, these were integrated in the “sealed areas” (Taha 1997; Wang et al. 2016).

2.4 Historical temperature data

Other than our recent measurements with a temporal resolution of 10 min at each location, the historical measurements gathered have far less data available each day. Since historical measurements required manual read out, most temperature

observations were scheduled to be checked at least three times a day. This was usually done in the morning, at noon, and in the evening, trying to capture daily minimum and maximum as well as a reasonable daily mean as best as possible. In the following, measurement procedures and calculations of daily means are detailed for individual historical periods in Brno.

Regarding the first station location H1 (period from 1800 to 1812, see Fig. 1 for locations), the provided data consists of daily values derived from the mean of five daily observations (Brázdil et al. 2006). For the next two measurement sites in the 1813–1847 period, either no values (H2) or no exact location and no values are reported (H3). In the period from 01/1848 to 12/1878 (H4 and H5), temperature was measured at 6 am, 2 pm, and 10 pm. Even though these times do not match exactly, a calculation of daily values was performed or conducted using the “Mannheimer Stunden.” Since 01/1879, measuring times were adopted to the “Mannheimer Stunden” 7 am, 2 pm, and 9 pm of mean local time, though recording shifted for a short period of time (06/1885–12/1889) to 6 am, 1 pm, and 9 pm. In this study, we did not analyze various methods of daily mean calculation. The otherwise continuous dataset contains a total of 207 days with missing or incorrect temperature values in the period from 1878 to 1890.

In order to quantify a possible bias from historical relocations, the current effect of land cover on local temperatures was assessed and linked with information derived from digitalized historical maps provided by the Moravian Land Archive, Brno, Czech Republic. Since only reliable information on buildings is shown on the historical maps, only this land cover type was digitalized. For each location of the historical measurement sites, a map was used which represents the respective building density (cf. Table 4). Building density in various radii (50 m, 100 m, 300 m, 500 m, 800 m, 1000 m) was determined for each time interval the stations experienced

a change in location. Under the assumption that the percentage of buildings in the respective radius of historical and current maps has hardly changed, the relationship between building cover and temperature variation established in the analysis of the current station network was used to remove the bias caused by the varying building cover at the historical measuring sites. Using equations for mean temperature in Table 3 and the percentage of buildings within the 500 m radius derived from historical maps, a bias was calculated per season, resulted due to building density. Since other types of land cover such as sealed areas or vegetation were not part of the historical maps, this analysis was exclusively based on building cover. Moreover, Dobrovolný et al. (2012) proved that the building density belongs to the best predictor of daily mean temperature in Brno with explained common variance ranging from 50 (winter) to 74% (spring).

3 Results

In order to identify a possible UHI effect, an overview on spatial temperature patterns is presented in Fig. 2. The overall largest differences among the station groups become apparent for mean and minimum temperatures in summer. Mean temperatures are significantly higher at urban sites compared to rural sites reaching 0.9 K in summer, 0.8 K in spring, and 0.6 K in autumn. Winter temperatures display the highest variability in the data, and differences among station types are almost negligible. Even though minimum temperatures are certainly characterized by a larger variability compared to mean temperatures, they emphasize the fact that rural areas are characterized by cooler conditions compared to the urban sites during all seasons (~1.2 K) except for winter. Since maximum temperatures did not display significant differences among the station groups and hence did not show any connection to land cover, it was disregarded from further analysis. Lower correlation of daily maximum temperatures to density

of buildings compared to daily mean and minimum temperatures was already reported by Dobrovolný et al. (2012). They analyzed these relationships for a set of days with radiation-driven weather with a clear sky and no advection. They argue that the maximum temperatures are more variable in highly heterogeneous urban environment. The same confirms Ho et al. (2014) analyzing variability of maximum land surface temperatures.

As a second step, Pearson's correlation between mean and minimum temperatures and the percentage of coverage of various land cover categories was performed, revealing several significant relations especially in the 300 m and 500 m radii (Fig. 3). For mean temperatures, the highest correlations among all land cover types were found for "building" when spring temperatures and a 100-m radius were considered ($R^2 = 0.72$). The inter-seasonal patterns are very similar, with larger radii leading to decreasing correlation strength, although remaining significant. The category "total vegetation" displays a significant relationship during all seasons but winter, even though seasonal R^2 values for categories of "low vegetation" and "high vegetation" did not exceed 0.4 when considered separately in a pre-analysis. With 500 m being the most influential radius, the highest coefficients of determination are again linked to temperatures in spring. Since "sealed areas" and "paved areas" revealed a very similar pattern compared to "building," these land cover classes were omitted from the figure.

For minimum temperatures, correlations are diverse in close vicinity of the stations, and they decrease if radii of more than 300 m are considered. The courses shown in Fig. 3 are almost identical throughout all seasons with spring and autumn displaying the highest values. Like mean temperatures, "building" category revealed significant correlations for all seasons (average $R^2 \sim 0.5$), although the explained variance is lower in minimum temperatures. Other than for mean temperatures, "sealed areas" and "paved areas" (not shown here) reveal similar patterns including significant correlations during all seasons in radii of 100 m and more. Regardless of the season, the coefficients of determination display peak values for the 100–500 m radii, and all correlations are significant if "total vegetation" is considered. A pre-analysis revealed this to be caused by a strong influence of "high vegetation," while "low vegetation" showed very low R^2 values compared to other parameters tested. Overall, correlation strength is lower than for mean temperatures with peak values of $R^2 = 0.6$.

Since building coverage is crucial for the determination of the relocation bias and correlations for mean and minimum temperatures were high during spring in the 500 m and 300 m radii, linear regression models presented in Fig. 4 served for the analysis applied to all seasons. We conclude that with an increase of the building cover by 10%, the average temperature simultaneously rises by 0.2 K with a very low variance at the same time. By comparison, minimum temperatures show

Table 3 Regression equations and R^2 values for land cover category "buildings" and temperature relation

	Mean temperature	
	Function	R^2
DJF	$y = 0.0087 \times + 0.82$	0.2
MAM	$y = 0.0205 \times + 10.37$	0.68**
JJA	$y = 0.0218 \times + 19.60$	0.57**
SON	$y = 0.0149 \times + 9.86$	0.46*
	Minimum temperature	
	Function	R^2
DJF	$y = 0.021 \times - 1.64$	0.56**
MAM	$y = 0.0349 \times + 4.70$	0.45*
JJA	$y = 0.0282 \times + 13.22$	0.36*
SON	$y = 0.0305 \times + 5.50$	0.47*

* $p < 0.05$; ** $p < 0.01$

Fig. 2 Seasonal air temperature variability based on daily data from June 2011 to February 2015 of rural ($n = 3$, left) as well as urban stations with 41–75% ($n = 6$, middle) and > 75% sealed areas ($n = 2$, right), respectively. Temperatures are displayed as anomalies, more specifically as differences to the mean of all sensors. Data exceeding 1.5 times the interquartile range are removed from whiskers and shown as outliers

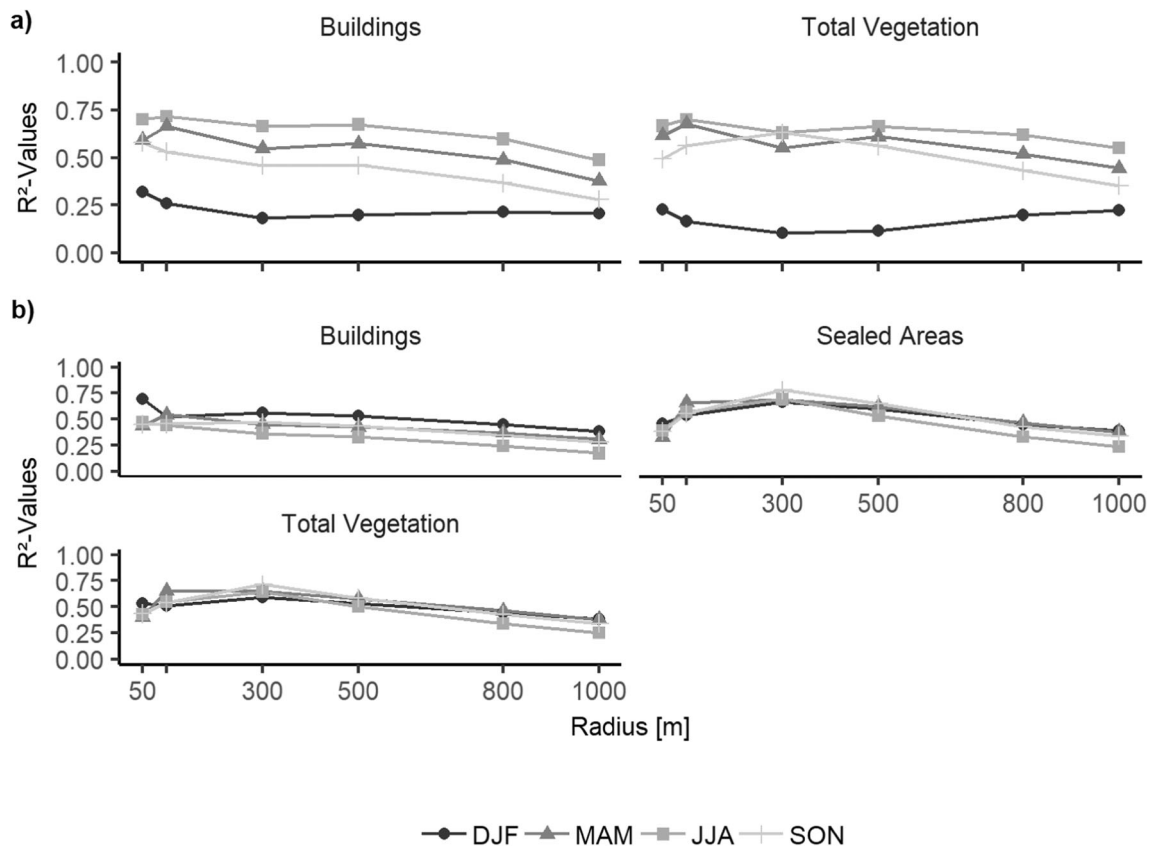
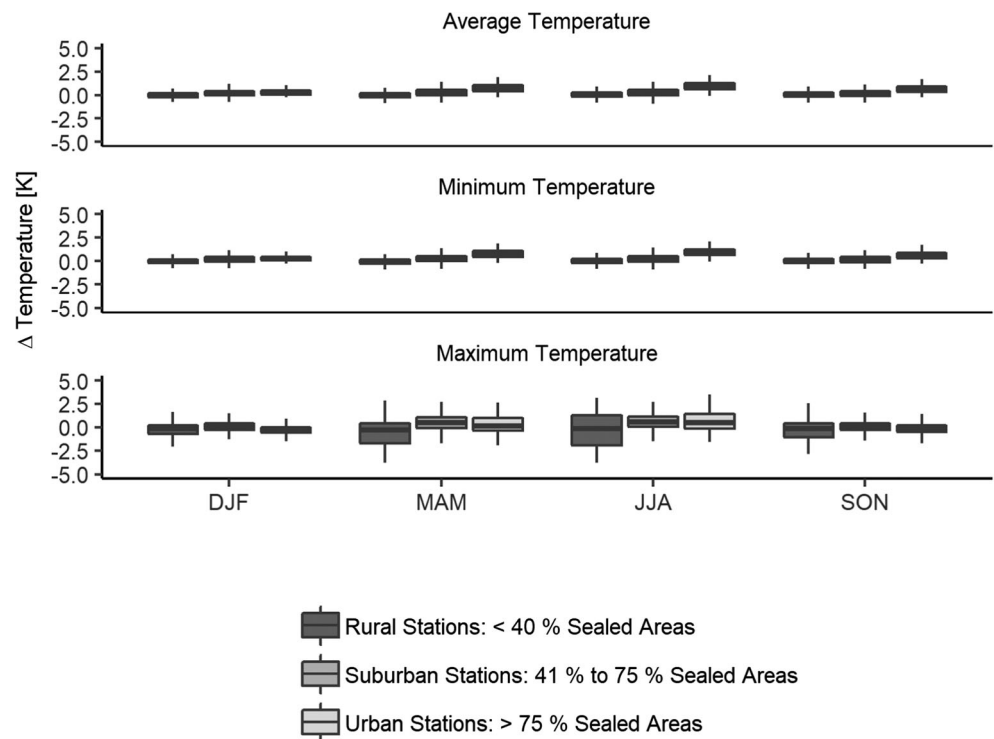
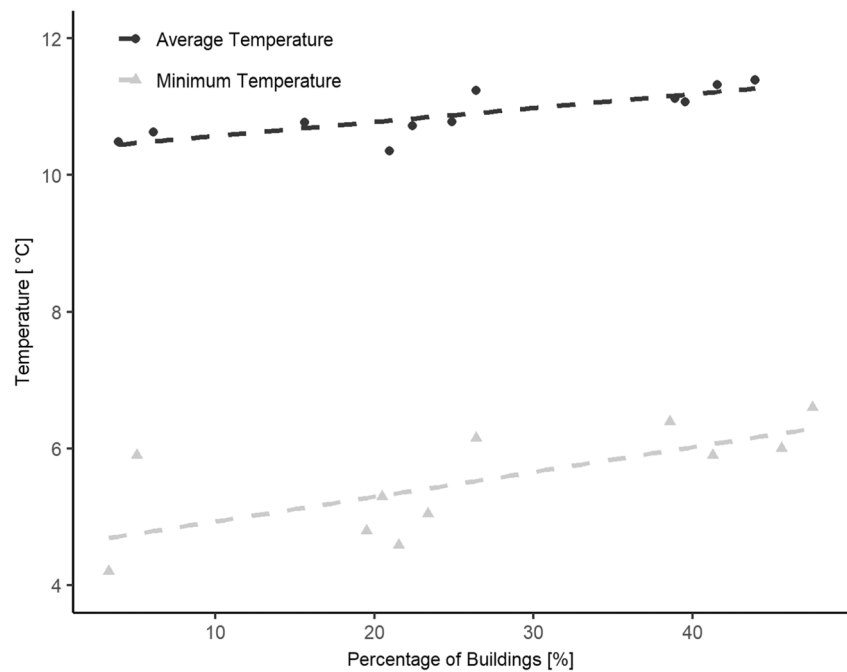


Fig. 3 Coefficients of determination for **a** seasonal average and **b** minimum temperatures correlated with selected types of land cover relative to different distances to the stations. Selection was based on the correlation strength and importance of each land cover for later analysis

Fig. 4 Regression analysis based on the relation between the percentage of built-up area within the station surroundings of 300 m radius and spring minimum temperature (R^2 value, 0.45) and 500 m radius and mean temperature (R^2 value, 0.67), respectively. Spring temperatures were selected due to exceptionally high R^2 values



increased variability but more intense temperature increases with increasing percentage of building cover (0.4 K/10% buildings). Table 3 summarizes the regression functions for every season as well as the correlation coefficients, revealing significant relations ($p < 0.05$). Mean temperatures display the strongest correlations, whereas the increase in temperature per % buildings is the highest in case of minimum temperatures. This confirms that the minima are controlled by additional warming caused by urban structures like latent heat storage in sealed surfaces and its release during night. Based on information about building density in individual historical periods, the equations compiled for the present situation were used to quantify the urban bias at each historical measurement site (Table 4). This approach enabled to correct measured temperatures during the corresponding time intervals.

With building density having the strongest relation to spring temperatures ($R^2 = 0.72$), Fig. 5 compares the original and adjusted mean spring temperatures as an example. The most striking is the fact that until 1890, the relocation bias is considerably higher than during any time later. Before 1890, the meteorological stations were established near the city center, where building density was relatively high (30% within a 500-m radius), especially biasing the first period from 1800 to 1812 at 0.66 K and the period from 1884 to 1890 at 0.59 K (cf. Table 4). The station was then moved to the periphery of the city after 1890, where building density was lower, reaching only 2–3% within a radius of 500 m and constraining the relocation bias to only 0.02 K.

Gradual shift of measurement sites from the more densely build-up center of historical town to less build-up sites is

Table 4 Overview of the historical measurement periods of the Brno meteorological station, together with the built fraction in a 500-m radius around the past measuring locations derived from historical maps drawn in the years listed in column three. Columns 4–8 display the quantified heat bias (in K) in different seasons caused by nearby buildings based on the equations shown in Table 3

Name	Duration	Map of year	Built fraction (500 m)	Bias DJF	Bias MAM	Bias JJA	Bias SON	
H 1	1800–1812	1824	32%	0.28	0.66	0.7	0.48	
H2	1813–1815; 1819	1824	30%	Missing temperature values				
H3	1819–1848	Missing temperature values and missing location information						
H 4	1848–1853	1858	18%	0.16	0.37	0.39	0.27	
H 5	1853–1878	1858	17%	0.15	0.35	0.37	0.25	
H 6	1878–1883	1909	17%	0.15	0.35	0.37	0.25	
H 7	1884–1890	1909	29%	0.25	0.59	0.63	0.43	
H 8	1890–1922	1929	2%	0.02	0.04	0.04	0.03	
H 9	1923–1960	1929	3%	0.03	0.06	0.07	0.04	
H 10	1961–2005	2013	3%	0.03	0.06	0.07	0.04	

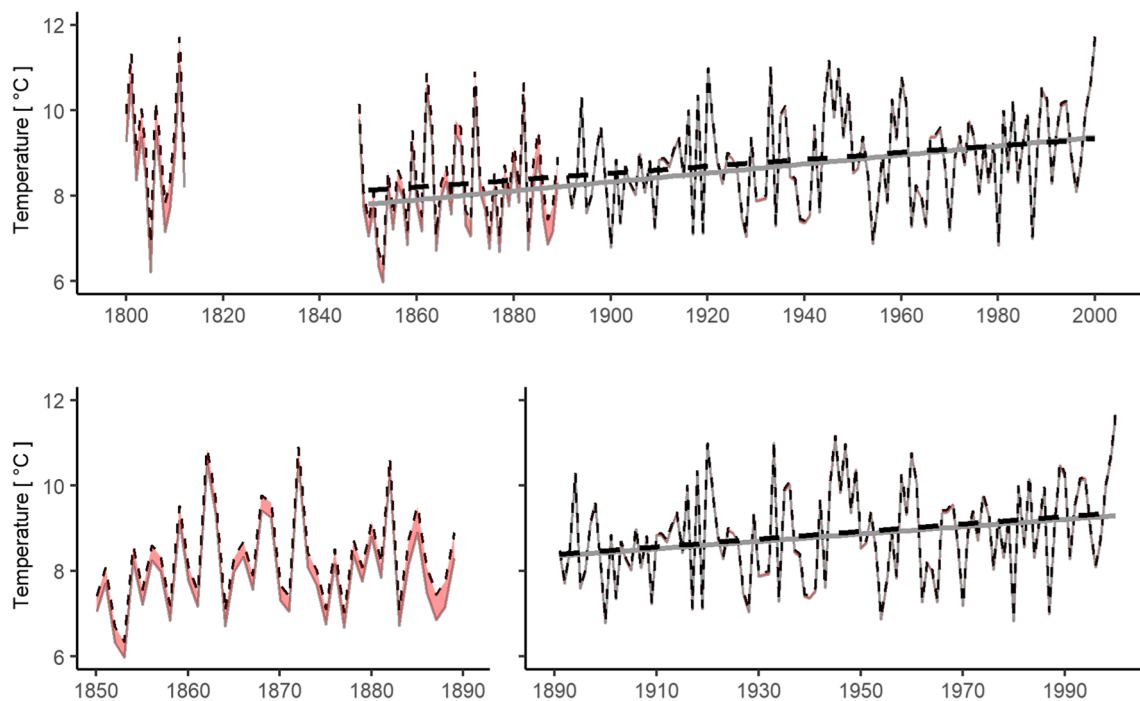


Fig. 5 Measured and corrected Brno MAM record from 1800 to 1812 and 1848 to 2000. Data from the nineteenth century (left) and twentieth century (right) are displayed separately to illustrate the strong corrections in the beginning and the minor changes in the later part. Spring season was selected due to the strongest relation to building density. Black,

dotted line indicates measured temperature, and gray line indicates corrected temperature; red coloration shows the difference between measured and corrected temperature. For the period 1813 to 1847, no data has been transmitted

responsible for the fact that the corrections increase the overall warming trend from 0.77 to 1.05 K/100 years. If the 1850–1900 interval is considered, the changes are even stronger reaching 0.96 K/100 years for the original and 1.34 °C/100 years for the corrected temperature series. As the temperature bias due to building cover is mainly negligible in the twentieth century, both time series line up closely during the past around 100 years (Fig. 5).

4 Discussion

This study reveals a distinct UHI in the city of Brno that is most pronounced in summer but persistent throughout the whole year. Warming was strongly related to building coverage and sealed areas, while vegetation provides significant cooling for urban temperatures. By employing a regression analysis for building density and temperatures, we applied a correction for the UHI intensity to the 150-year Brno meteorological measurements to eliminate the influence of relocations. In the following section, we explain the patterns and intensities of the UHI in different seasons as well as its connection to various types of land cover, followed by a discussion of the relocation bias during different periods and its removal, as well as a comparison between the corrected and original time series.

4.1 Temperatures and their connection to settlement structure

A distinct UHI effect was found in Brno, with greatest contrasts between urban and rural temperatures detected during summer in mean and minimum temperatures and overall minor effects during winter. These seasonal variations are also reported from other cities like Hania, Greece, and Melbourne, Australia (e.g., Kolokotsa et al. 2009; Morris et al. 2001), though some climate conditions yield inverted situations (Yang et al. 2013). As suggested by Giridharan et al. (2007), the seasonal pattern can be explained by stronger summertime solar radiation amplifying the heating effect of urban materials and geometry. In addition, higher wind speeds and cloudy weather usually prevent the formation of a strong and long-lasting UHI in winter; however, minor warming could still be detected as is true for London (Giridharan and Kolokotroni 2009). For the city of Basel, Switzerland, Wicki et al. (2018) developed a multiple linear regression model with predictors from different data sources to model the urban air temperature distribution in order to predict the nightly UHI. Our results revealed the necessity of eliminating relocation biases in Brno considering different seasons.

Apart from these seasonal changes, the most distinct urban warming influence in minimum temperatures is in line with other studies. Kalnay and Cai (2003) report minimum

temperature trends in the USA to be most affected due to urbanization, and studies from Nanjing (Huang et al. 2008) or New York (Gaffin et al. 2008) support a decline in UHI intensity after sunrise. The main reason for this is energy, which was stored during the day through solar radiation and remains longer in the city due to multiple release heat and uptake processes of the now emerged sensible heat as well as anthropogenic heat sources (Oke 1982; Taha 1997).

Land cover was used to identify the structures and surfaces contributing most to cooling and warming, respectively. Overall, temperatures were strongly and significantly correlated with buildings, sealed areas, and vegetation. These findings confirmed source areas to influence radii of up to 1000 m as also found in other studies (e.g., Lindén et al. 2015). Correlation coefficients tended to decrease with increasing distance from the measurement locations. The strengths of correlations varied with season, with lowest influence of land cover in winter. Regression analysis shows that with increasing fraction of vegetated area, the temperature becomes lower. This is likely due to shading and evaporative cooling, which is most pronounced during the warmer months (Dimoudi and Nikolopoulou 2003; Weng et al. 2004). In contrast, the thermal properties of paved areas and buildings cause higher temperatures in their surroundings, generally most effective during summer when solar radiation is strongest (e.g., Lo and Quattrochi 2003). Both factors, low evapotranspiration and limited solar radiation, explain the weak correlation values in the cold season.

4.2 The relocation bias

The quantification of the relocation bias and hence the quality of the correction is determined by mainly two different factors: the dependence of temperatures on building density, and the representativeness and reliability of the current measurements. In the previous section, we showed that spatial temperature differences are significantly related to land cover, with buildings and sealed areas explaining most of the additional warming at urban sites. As this analysis is based on more than 1300 days of high-resolution data from 11 stations in and around Brno, we value the dataset to be very robust. As no significant changes were found in historical building cover compared to today, the current analysis is likely representative for the past 150 years. Being preserved as a site of historical importance, this is particularly true for the city center, where most relocations took place. However, in the vicinity of the station locations H8 and H9, at the border of the city, several new buildings have been constructed in the course of urban growth population increase. We assume the influence of these changes to be negligible, however, since the percentage of buildings rose by less than 7% in the surroundings of sites H8 and H9.

Other uncertainties arise from the historical maps. Since vegetation and surface cover were rarely included, only building cover could be used to assess the warming bias. This problem is likely less significant as only few areas were paved in the nineteenth century and, after that, the station moved to locations with almost no sealed and built-up surfaces.

Another aspect in cities is the concern of a possible anthropogenic warming due to direct heating effects. Even though most houses are heated in the winter season today, only a fraction of heat is emitted due to good insulation. In contrast, only minor insulation materials were used in former times allowing a great part of the heat to be transferred through the walls and windows to the outside. Consequently, Bozsaky (2011) assumes the influence of heating to be relatively balanced over time as the amount of heating was much lower 200 years ago. Nevertheless, this is an important issue especially during the nineteenth century when the station was installed in substantially urbanized areas, emphasizing the need to concentrate on the possible impact in further studies.

4.3 Time series correction

When dealing with long temperature series, other issues than relocations that might have had an impact on the historical measurements need to be considered. In particular, these are changes in the instrumentation and sheltering, in observing times and temperature mean calculations (e.g., Böhm et al. 2009). Since 1799, more sophisticated instruments were introduced and replaced by new ones several times. The impact of these changes on the data is hard to quantify, because information on exact dates is missing. For other changes, historical evidence is existent, e.g., a shift in recording daily maximum values (Brázdil et al. 2006). Since this change took place before 1850, it does not influence the later part of the record chosen for correction. Varying observing times and mean calculations (see chapter 2.5) could have an impact on data (Erk 1883; Valentin 1901), but might also be negligible as Moberg and Bergström (1997) pointed out for a temperature dataset from Sweden. Such influences are, however, generally difficult to estimate if parallel measurements are not available. Despite not being able to account for all these possible impacts and uncertainties, other studies detailed relocations to be the most severe influence in long temperature records (e.g., Syrakova and Stefanova 2008; Tuomenvirta 2001). Hence, by addressing them, we offer an improvement for the dataset. Nevertheless, further studies need to be carried out in order to include additional correction for less severe biases resulting from further interferences other than relocations.

Applying the correction causes minimum and mean temperatures to drop regardless of the season, as all historical locations were affected by a varying number of nearby buildings and hence by a corresponding warm bias. The larger corrections in the early part of the record during the second

part of the nineteenth century were necessary because measurements took place in the center and surrounding building density was high. This situation changed with the relocation in 1890, moving the station to a location almost free of built-up surfaces. Reducing the early temperature values led to an increase in the overall warming trend, a common effect after applying a homogenization to long station records (Begert et al. 2005; Brunet et al. 2006a). The twentieth century warming remains almost un-affected though, as building cover did not exceed 3% in the stations' vicinity and changes to the time series remained marginal after 1890. A comparable study by Dienst et al. (2017) of a 150-yearlong record from Sweden showed similar results. In consequence, the results insinuate that warming has been underestimated. However, Zhang et al. (2014) offer another explanation for these findings, stating that a correction for relocation biases typically increases warming trends, since the gradual warming due to urbanization is recovered. Relocating the station to more rural surroundings towards today lowers temperatures because of the decrease in nearby buildings and sealed surface. Therefore, this procedure weakens the otherwise increasing background warming inherent in the time series due to city growth. According to them, by removing all influences only connected to warming by nearby land cover, this background urban warming is still present in the time series.

5 Conclusion

A consistent UHI effect was found in an extensive dataset comprised of more than 1300 days of high-resolution data from 11 stations in and around Brno. The UHI effect was most pronounced in summer minimum temperatures. To answer the question whether historical measurements in the city have been affected by this, a correlation of the recent temperature data and various types of land cover was performed, revealing sub-regional warming to be strongly and significantly correlated with built-up areas, especially in radii of 300 to 500 m. This relation was used to assess the warming bias at different historical measurement sites based on historical maps documenting the built areas in the past. Our analyses showed that the long temperature record from Brno is substantially biased in the nineteenth century when measurements took place at various sites within the city center. This situation changed in the twentieth century with the station moving out of the center. Hence, removing the relocation bias from the dataset considerably lowers temperatures in the nineteenth century. An elimination of the relocation bias in long-term temperature records using the approach presented here is feasible only if a dense network of recent temperature is established and sufficient historical information on the original measurement sites and conditions are available. Even though other factors were excluded from this correction

approach, this study clearly documents the severity of non-climatic, anthropogenic influences in one of the longest meteorological records from Europe while at the same time proving its reliability in the twentieth century.

Publisher's note Springer Nature remains neutral with regard to jurisdictional claims in published maps and institutional affiliations.

References

- Aguilar E, Auer I, Brunet M, Peterson TC, Wieringa J (2003) Guidelines on climate metadata and homogenization WMO/TD 1186
- Allen L, Lindberg F, Grimmond CSB (2011) Global to city scale urban anthropogenic heat flux: model and variability. *Int J Climatol* 31: 1990–2005
- Arnfield AJ (2003) Two decades of urban climate research: a review of turbulence, exchanges of energy and water, and the urban heat island. *Int J Clim* 23:1–26. <https://doi.org/10.1002/joc.859>
- Auer I et al (2005) A new instrumental precipitation dataset for the greater alpine region for the period 1800–2002. *Int J Clim* 25:139–166. <https://doi.org/10.1002/joc.1135>
- Auer I et al (2007) HISTALP—historical instrumental climatological surface time series of the Greater Alpine Region. *Int J Clim* 27: 17–46. <https://doi.org/10.1002/joc.1377>
- Begert M, Schlegel T, Kirchhofer W (2005) Homogeneous temperature and precipitation series of Switzerland from 1864 to 2000. *Int J Climatol* 25:65–80
- Böhm R, Jones PD, Hiebl J, Frank D, Brunetti M, Maugeri M (2009) The early instrumental warm-bias: a solution for long central European temperature series 1760–2007. *Clim Chang* 101:41–67. <https://doi.org/10.1007/s10584-009-9649-4>
- Bozsaky D (2010) The historical development of thermal insulation materials. *Periodica Polytechnica Architecture* 41(2):49
- Brázdil R, Řezníčková L, Valášek H (2006) Early instrumental meteorological observations in the Czech lands I: Ferdinand Knittelmayer, Brno, 1799–1812. *Meteorologický časopis* 9:59–71
- Brunet M et al (2006a) A case-study/guidance on the development of long-term daily adjusted temperature datasets WMO/TD 1425
- Brunet M et al (2006b) The development of a new dataset of Spanish Daily Adjusted Temperature Series (SDATS) (1850–2003). *Int J Climatol* 26:1777–1802. <https://doi.org/10.1002/joc.1338>
- Chen X-L, Zhao H-M, Li P-X, Yin Z-Y (2006) Remote sensing image-based analysis of the relationship between urban heat island and land use/cover changes. *Remote Sens Environ* 104:133–146
- Chow W, Roth M (2006) Temporal dynamics of the urban heat island of Singapore. *Int J Clim* 26:2243–2260. <https://doi.org/10.1002/joc.1364>
- Cox PM, Betts RA, Bunton CB, Essery RLH, Rowntree PR, Smith J (1999) The impact of new land surface physics on the GCM simulation of climate and climate sensitivity. *Clim Dyn* 15:183–203. <https://doi.org/10.1007/s003820050276>
- Dienst M, Lindén J, Engström E, Esper J (2017) Removing the relocation bias from the 155-year Haparanda temperature record in northern Europe. *Int J Climatol* 37:4015–4026. <https://doi.org/10.1002/joc.4981>
- Dimoudi A, Nikolopoulou M (2003) Vegetation in the urban environment: microclimatic analysis and benefits. *Energ Buildings* 35:69–76
- Dobrovolný P et al (2012) *Klima Brna. Víceúrovňová analýza městského klimatu*. Brno

- Erk F (1883) Die Bestimmung wahrer Tagesmittel der Temperatur unter besonderer Berücksichtigung langjähriger Beobachtungen von München. Verl. d. Akad. München 1883. Abhandlungen: Bd. 14, Abth. 2 = [9]
- Esper J, Frank D, Büntgen U (2007) On selected issues and challenges in dendroclimatology. In: Kienast F, Wildi O, Ghosh S (eds) A changing world: challenges for landscape research. Springer, Berlin, pp 113–132
- Gaffin SR et al (2008) Variations in New York city's urban heat island strength over time and space. *Theor Appl Climatol* 94:1–11. <https://doi.org/10.1007/s00704-007-0368-3>
- Giridharan R, Kolokotroni M (2009) Urban heat island characteristics in London during winter. *Sol Energy* 83:1668–1682. <https://doi.org/10.1016/j.solener.2009.06.007>
- Giridharan R, Lau SSY, Ganesan S, Givoni B (2007) Urban design factors influencing heat island intensity in high-rise high-density environments of Hong Kong. *Build Environ* 42:3669–3684. <https://doi.org/10.1016/j.buildenv.2006.09.011>
- Goodridge JD, (1992) Urban bias influences on long-term California air temperature trends. *Atmospheric Environment. Part B. Urban Atmosphere* 26 (1):1–7. [https://doi.org/10.1016/0957-1272\(92\)90032-n](https://doi.org/10.1016/0957-1272(92)90032-n)
- Hart MA, Sailor DJ (2009) Quantifying the influence of land-use and surface characteristics on spatial variability in the urban heat island. *Theor Appl Climatol* 95:397–406. <https://doi.org/10.1007/s00704-008-0017-5>
- Ho HC et al (2014) Mapping maximum urban air temperature on hot summer days. *Remote Sens Environ* 154:38–45
- Huang L, Li J, Zhao D, Zhu J (2008) A fieldwork study on the diurnal changes of urban microclimate in four types of ground cover and urban heat island of Nanjing, China. *Build Environ* 43:7–17. <https://doi.org/10.1016/j.buildenv.2006.11.025>
- Jones PD, Lister D, Li Q (2008) Urbanization effects in large-scale temperature records, with an emphasis on China. *J Geophys Res* 113:1–12
- Kalnay E, Cai M (2003) Impact of urbanization and land-use change on climate. *Nature* 423:528–531
- Kolokotsa D, Psomas A, Karapidakis E, (2009) Urban heat island in southern Europe: the case study of Hania, Crete. *Solar Energy* 83(10):1871–1883. <https://doi.org/10.1016/j.solener.2009.06.018>
- Leach AJ (2007) The climate change learning curve. *J Econ Dyn Control* 31:1728–1752. <https://doi.org/10.1016/j.jedc.2006.06.001>
- Li RM, Roth M (2009) Spatial variation of the canopy-level urban heat island in Singapore. Paper presented at the seventh International Conference on Urban Climate, Yokohama, Japan
- Lindén J (2011) Nocturnal cool island in the Sahelian city of Ouagadougou, Burkina Faso. *Int J Climatol* 31:605–620
- Lindén J, Esper J, Holmer B (2015) Using land cover, population, and night light data for assessing local temperature differences in Mainz, Germany. *J Appl Meteorol Climatol* 54:658–670
- Lo CP, Quattrochi DA (2003) Land-use and land-cover change, urban heat island phenomenon, and health implications: a remote sensing approach. *Photogramm Eng Remote Sens* 69:1053–1063
- Moberg A, Bergström H (1997) Homogenization of Swedish temperature data - part III - the long temperature records from Uppsala and Stockholm. *Int J Climatol* 17:667–699
- Morris CJG, Simmonds I, Plummer N (2001) Qualification of the influences of wind and cloud on the nocturnal urban heat island of a large city. *J Appl Meteorol* 40:169–182
- Oke TR (1982) The energetic basis of the urban heat island. *Q J R Meteorol Soc* 108:1–24
- Parker DE (2010) Urban heat island effects on estimates of observed climate change. *Wiley Interdiscip Rev Clim Chang* 1(1):123–133
- Peel MC, Finlayson BL, McMahon TA (2007) Updated world map of the Köppen-Geiger climate classification. *Hydrol Earth Syst Sci Discuss EGU* 11:1633–1644
- Pérez-Zanón N, Sigró J, Domonkos P, Ashcroft L (2015) Comparison of HOMER and ACMANT homogenization methods using a central Pyrenees temperature dataset. *Adv Sci Res* 12:111–119. <https://doi.org/10.5194/asr-12-111-2015>
- Portman DA (1993) Identifying and correcting urban bias in regional time series: surface temperature in China's Northern Plains. *J Climate* 6: 2298–2308. [https://doi.org/10.1175/1520-0442\(1993\)006<2298:iacubi>2.0.co;2](https://doi.org/10.1175/1520-0442(1993)006<2298:iacubi>2.0.co;2)
- Rahimzadeh F, Zavareh MN (2014) Effects of adjustment for non-climatic discontinuities on determination of temperature trends and variability over Iran. *Int J Climatol* 34:2079–2096
- Štěpánek P, Zahradníček P, Skalák P (2009) Data quality control and homogenization of air temperature and precipitation series in the area of the Czech Republic in the period 1961–2007. *Adv Sci Res* 3:23–26. <https://doi.org/10.5194/asr-3-23-2009>
- Stewart ID, Oke TR (2012) Local climate zones for urban temperature studies. *Bull Am Meteorol Soc* 93:1879–1900. <https://doi.org/10.1175/bams-d-11-00019.1>
- Syrakova M, Stefanova M (2008) Homogenization of Bulgarian temperature series. *Int J Climatol* 29:1835–1849
- Taha H (1997) Urban climates and heat islands: albedo, evapotranspiration, and anthropogenic heat. *Energ Buildings* 25:99–103
- Tuomenvirta H (2001) Homogeneity adjustments of temperature and precipitation series - Finnish and Nordic data. *Int J Climatol* 21:495–506
- Unwin DJ (1980) The synoptic climatology of Birmingham's urban heat island, 1965–74. *Weather* 35:43–50
- Valentin J (1901) Der tägliche Gang der Lufttemperatur in Österreich Veröffentlichungen des Preußischen Meteorologischen Instituts 254
- Venema V et al (2012a) Benchmarking homogenization algorithms for monthly data. *Clim Past* 8:89–115
- Venema V et al (2012b) Detecting and repairing inhomogeneities in datasets, assessing current capabilities. *Bull Am Meteorol Soc* 93: 951–954
- Vincent LA (1998) A technique for the identification of inhomogeneities in Canadian temperature series. *J Climate* 11:1094–1104. [https://doi.org/10.1175/1520-0442\(1998\)011<1094:atfio>2.0.co;2](https://doi.org/10.1175/1520-0442(1998)011<1094:atfio>2.0.co;2)
- Voldoire A et al (2012) The CNRM-CM5.1 global climate model: description and basic evaluation. *Clim Dyn* 40:2091–2121. <https://doi.org/10.1007/s00382-011-1259-y>
- Wang ZH, Zhao X, Yang J, Song J (2016) Cooling and energy saving potentials of shade trees and urban lawns in a desert city. *Appl Energy* 161:437–444. <https://doi.org/10.1016/j.apenergy.2015.10.047>
- Weng Q, Lu D, Schubring J (2004) Estimation of land surface temperature–vegetation abundance relationship for urban heat island studies. *Remote Sens Environ* 89:467–483. <https://doi.org/10.1016/j.rse.2003.11.005>
- Wicki A, Parlow E, Feigenwinter C (2018) Evaluation and modeling of urban heat island intensity in Basel, Switzerland. *Climate* 6(3):55
- Wigley TML, Santer BD (2013) A probabilistic quantification of the anthropogenic component of twentieth century global warming. *Clim Dyn* 40:1087–1102. <https://doi.org/10.1007/s00382-012-1585-8>
- Yang P, Ren G, Liu W (2013) spatial and temporal characteristics of Beijing urban heat island intensity. *J Appl Meteorol Climatol* 52: 1803–1816
- Yokobori T, Ohta S (2009) Effect of land cover on air temperatures involved in the development of an intra-urban heat island. *Clim Res* 39:61–73. <https://doi.org/10.3354/cr00800>
- Zhang L, Ren G, Ren Y, Zhang A, Chu Z, Zhou Y (2014) Effect of data homogenization on estimate of temperature trend: a case of Huairou station in Beijing municipality. *Theor Appl Climatol* 115:365–373
- Zhen L and Zhong-Wei Y (2015) Homogenized Daily Mean/Maximum/Minimum Temperature Series for China from 1960–2008. *Atmospheric and Oceanic Science Letters* 2(4):237–243